Large-scale first-principles molecular dynamics for electrochemical systems with O(N) methods

Tsukuru Ohwaki, Minoru Otani, Tamio Ikeshoji, and Taisuke Ozaki

Citation: J. Chem. Phys. **136**, 134101 (2012); doi: 10.1063/1.3698583
View online: http://dx.doi.org/10.1063/1.3698583
View Table of Contents: http://jcp.aip.org/resource/1/JCPSA6/v136/i13
Published by the American Institute of Physics.

Large-scale first-principles molecular dynamics for electrochemical systems with O(*N*) methods

Tsukuru Ohwaki,[1] Minoru Otani,[2] Tamio Ikeshoji,[2,3] and Taisuke Ozaki[4]
[1]*NISSAN Research Center, 1 Natsushima-cho, Yokosuka, Kanagawa 237-8523, Japan*
[2]*Nanosystem Research Institute, National Institute of Advanced Industrial Science and Technology (AIST), Tsukuba, Ibaraki 305-8568, Japan*
[3]*Advanced Institute for Materials Research, Tohoku University, 2-1-1 Katahira, Aoba-ku, Sendai, Miyagi 980-8577, Japan*
[4]*Research Center for Integrated Science (RCIS), Japan Advanced Institute of Science and Technology (JAIST), 1-1 Asahidai, Nomi, Ishikawa 923-1292, Japan*

(Received 6 October 2011; accepted 13 March 2012; published online 2 April 2012)

A method for large-scale first-principles molecular dynamics (MD) simulations on electrochemical systems has been developed by combining the effective screening medium (ESM) method with O(*N*) density functional theory (DFT). This implementation has been significantly simplified by the introduction of neutral atom potentials, which minimizes the modifications to existing DFT code. In order to demonstrate ability of this implementation, it has been applied to an electrochemical system consisting of a H-Si(111) electrode, which is a candidate anode for high-capacity Li-ion secondary batteries, and a propylene carbonate (PC) solvent to simulate how PC molecules in the vicinity of the electrode surface respond to an imposed electric field. The large-scale MD simulation clearly demonstrates that the combination of the ESM and O(*N*) DFT methods provides a useful tool for first-principles investigation of complicated electrochemical systems such as high-capacity batteries.
 [http://dx.doi.org/10.1063/1.3698583]

I. INTRODUCTION

A first-principles method capable of giving meaningful results under an electric bias would be of great use in the investigation of electrochemical reactions in secondary cells such as in the lithium-ion (Li-ion) battery. A better understanding of the microscopic mechanisms of the electrochemical reactions is not just of academic interest, but would aid in the design of high-performance battery systems. A key issue in such a simulation of an electrochemical system, where the simulation cell is under conditions close to those in an experiment, is to develop a method which allows us to apply an electric bias to the system as occurs with an electrode and an electrolyte solution. Otani and Sugino have recently developed a new first-principles computational method to have charged or biased surface-interface systems consisting of a slab,[1] and the method has been used to simulate the hydrogen electrode in water electrolysis and fuel cells.[2,3] In their approach, the electric bias is controlled by doping excess charge in the target electrode with the appropriate boundary conditions guaranteeing the charge neutrality. Such boundary conditions are introduced through Poisson's equation, which is equivalent to placing a medium having a certain dielectric constant (effective screening medium (ESM)).[1] Charge separation (electrical double layer) in an electrochemical system can be modeled using ESMs with two semi-infinite media, vacuum (relative permittivity $\varepsilon = 1$) and an ideal metal ($\varepsilon = \infty$), located on either side of a unit cell, as shown in Fig. 1. Electrical double layer was also modeled in the first-principles calculations by Neurock *et al.*,[4] in which a uniform background charge is introduced as a counter charge of the doped excess one. However, while the interaction of the background charge with the charge on the electrode is somehow uncertain in this scheme, electric double layer between the electrode and the solution is more naturally modeled in the ESM scheme.

Although the ESM method provides a very useful scheme to simulate reactions under a bias, it is still a challenge to perform MD simulations for electrochemical systems that have large solvent molecules, as in Li-ion batteries, because the systems are just too big. Since the computational effort for most first-principles methods scales with the cube of the system size, applying the ESM method to such large-scale systems will be hampered by the computational cost. In this paper, we have developed a method which combines ESM with O(*N*) density functional theory (DFT) based on the O(*N*) Krylov subspace method[5] and optimized localized atomic basis functions.[6] This should extend the ESM method to large systems and enable us to address more challenging electrochemical phenomena. By assuming the bandgap in an electrochemical system may approach zero under a bias, the O(*N*) method combined with ESM should be applicable not only to insulators but also to metals. Among the O(*N*) methods developed so far, the O(*N*) Krylov subspace method is one of the very few applicable to insulators and metals in a single framework.[5] Thus, the combination of O(*N*) Krylov subspace with the ESM method can guarantee the method's applicability to a wide variety of systems regardless of the bandgap. Implementation of the ESM method is significantly simplified by the introduction of the neutral atom potential (NAP) method[7–9] regardless of the basis functions used. A modification to existing DFT codes using the NAP method is required only for Poisson's equation solver in the code and no

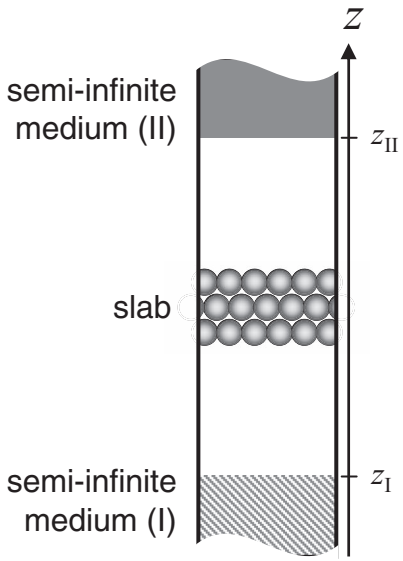

FIG. 1. Schematic view of a slab with ESM boundaries. In simulations of an electrode–solvent interface, semi-infinite vacuum ($\varepsilon = 1$) and ideal metal ($\varepsilon = \infty$) media were placed at $z = z_I$ and z_{II}, respectively.

change is required for the calculation of forces on atoms. This is a superior method to the original implementation presented in Ref. 1. Since the NAP method has been widely used for O(N) DFT codes,[7–10] this simplified implementation of the ESM method can be immediately utilized in existing DFT codes. Recent advances in the optimization of atomic basis functions have improved their accuracy,[6,11–13] so that interactions between electrodes and ions/molecules and between ions and molecules can be accurately treated without suffering from a basis set superposition error (BSSE). Our implementation adopts pseudo-atomic orbitals (PAO) as basis functions of which the radial shape has undergone variational optimization, assuring that the BSSE has been significantly reduced.[14]

This paper is organized as follows: In Sec. II, the ESM method is briefly introduced and the implementation of the ESM method is presented for a first-principles calculation scheme based on the NAP method and PAO basis functions. In Sec. III, a series of benchmark calculations for simple systems are shown to validate the accuracy of our method in comparison with results by other methods. In Sec. IV, in order to show the ability of our scheme, a large-scale first-principles MD calculation was carried out for the interface between a H-terminated Si(111) electrode and propylene carbonate (PC) solvent under an electric field. Si–PC is one of the possible combinations between a Si-based anode and solvent in a Li-ion secondary cell. A summary of the developed method, conclusion, and future perspectives are given in Sec. V.

II. APPLICATION OF THE ESM METHOD TO PAO AND NAP-BASED SCHEME

A. ESM method

In a simulation of an interface between an electrode and electrolyte solution under periodic boundary conditions based on the ESM method, a slab representing the interface is bound between two semi-infinite media (ESMs), vacuum (relative permittivity $\varepsilon = 1$) and an ideal metal ($\varepsilon = \infty$) as shown in Fig. 1. Those media are located at $z < z_I$ and $z > z_{II}$, respectively. An electric bias can be imposed by doping excess charge into the system, in which the electrode generally accumulates the charge. The semi-infinite metal medium has the corresponding mirror charge to keep the charge neutrality. Due to the electrostatic interaction between the doped and the mirror charges, the charge in the electrode is accumulated on the solution side, giving the same situation as at an actual electrode surface, i.e., electric double layer.

The total energy E_{tot} of the system under the boundary conditions with respect to the electrostatic interactions is expressed using Green's function G for Poisson's equation as follows:

$$E_{tot}[n] = K[n] + E_{ex}[n] + \frac{1}{2}\int\int d\mathbf{r}d\mathbf{r}' n_{tot}(\mathbf{r})\, G(\mathbf{r},\mathbf{r}')n_{tot}(\mathbf{r}'), \quad (1)$$

where n denotes the electron density and n_{tot} is the total charge density, the sum of n and n_c, the core charge density. K and E_{ex} represent the kinetic and exchange-correlation energy functionals of n, respectively. The third term is the electrostatic interaction energy, expressing that charges at different points, $\mathbf{r}$ and $\mathbf{r}'$, interact with each other through $G(\mathbf{r},\mathbf{r}')$. Green's function for the combination of the two boundaries, the vacuum and metal media, is obtained analytically,[1,15] and is introduced into Eq. (1) to calculate the total energy of the system. Thus, it should be noted that only the Poisson's equation solver has to be modified in the implementation of the ESM method.

B. NAP method

When electronic and core charges are treated separately in Poisson's equation solver, in principle a separate Green's function should be used for each of three Poisson's equations for electron–electron, electron–core, and core–core interactions with different formulations. For the electron–core interaction, it is necessary to change the long-range term associated with the interaction between electronic and effective core charges. For the core–core interaction, the Ewald summation should be reformulated according to which ESMs have been introduced.[1] On the other hand, when a simultaneous treatment of electronic and core charges is employed in Poisson's equation solver, one can reduce long-range electrostatic interactions to a single term. In this case, the ESM method is simply introduced into the code by modifying only this long-range interaction term.

The NAP method[7–9] is one such scheme to deal with electronic and core charges simultaneously[16] within norm-conserving pseudopotential schemes.[17,18] In this method, the electronic structure is calculated from the difference electron charge density, $\delta n(\mathbf{r})$, defined at point $\mathbf{r}$ as

$$\delta n(\mathbf{r}) = n(\mathbf{r}) - n^{(a)}(\mathbf{r}) = n(\mathbf{r}) - \sum_k n_k^{(a)}(\mathbf{r}), \quad (2)$$

where $n(\mathbf{r})$ denotes the electron density, and $n^{(a)}{}_k(\mathbf{r})$ is an atomic electron density associated with the kth atom. The atomic electron density $n^{(a)}{}_k(\mathbf{r})$ is generated in advance by solving atomic Kohn–Sham (KS) equations under a confinement potential with a cutoff radius $r_{c,k}$.[7–9] In addition, $n^{(a)}(\mathbf{r})$ is a superposition of $n^{(a)}{}_k(\mathbf{r})$ for all the atoms. By adopting this treatment, the sum of the long-range Coulomb interaction energy terms, $E_{ec} + E_{ee} + E_{cc}$ (electron–core, electron–electron, and core–core Coulomb energies, respectively), can be transformed into a more tractable form without any approximation as follows:[7–9]

$$E_{ec} + E_{ee} + E_{cc} = E_{na} + E_{scc} + E_{\delta ee} \tag{3}$$

with

$$E_{na} = \int d\mathbf{r} n(\mathbf{r}) \sum_k V_{na,k}(\mathbf{r} - \mathbf{R}_k), \tag{4}$$

$$E_{scc} = \frac{1}{2} \sum_{k,l} \left(\frac{Z_k Z_l}{|\mathbf{R}_k - \mathbf{R}_l|} - \int d\mathbf{r} n_k^{(a)}(\mathbf{r} - \mathbf{R}_k) V_{H,l}^{(a)}(\mathbf{r} - \mathbf{R}_l) \right), \tag{5}$$

$$E_{\delta ee} = \frac{1}{2} \int d\mathbf{r} \delta n(\mathbf{r}) \delta V_H(\mathbf{r}), \tag{6}$$

where $V_{na,k}$ is a NAP constructed by the sum of the Hartree potential $V^{(a)}{}_{H,k}$ associated with the atomic electron density $n^{(a)}{}_k$ and the local part of the norm-conserving pseudopotential of the kth atom, $V_{core,k}$,

$$V_{na,k}(\mathbf{r}) = V_{H,k}^{(a)}(\mathbf{r}) + V_{core,k}(\mathbf{r}), \tag{7}$$

and $V^{(a)}{}_H$ and δV_H are the Hartree potential and its difference, respectively, as defined by

$$V_H^{(a)}(\mathbf{r}) = \sum_k V_{H,k}^{(a)}(\mathbf{r} - \mathbf{R}_k) = \sum_k \int d\mathbf{r}' \frac{n_k^{(a)}(\mathbf{r})}{|\mathbf{r} - \mathbf{r}'|}, \tag{8}$$

$$\delta V_H(\mathbf{r}) = \int d\mathbf{r}' \frac{\delta n(\mathbf{r})}{|\mathbf{r} - \mathbf{r}'|}. \tag{9}$$

The NAP energy E_{na} and screened core–core Coulomb energy E_{scc} are major contributors to the short-range interactions, and are not changed by the ESM boundaries in the calculation system as explained below.

The NAP $V_{na,k}$ is constructed from the spherical atomic electron density $n^{(a)}{}_k$, and is zero beyond $r_{c,k}$ due to Gauss's law. $V_{na,k}$ is, therefore, a short-range spherical potential, and is not affected by the ESM boundaries because the position of every atom is set far from the ESMs.[19]

E_{scc} is evaluated only from its neighboring atoms because the second term in Eq. (5) is exactly equivalent to the first term in Eq. (5) when $r_{c,k} + r_{c,l} \leq |\mathbf{R}_k - \mathbf{R}_l|$, and therefore, the long-range terms in Eq. (5) vanish. Out of the region of $r_{c,k}$, the spherical atomic electron density $n^{(a)}{}_k$ can be treated as a point charge with the same center. Its mirror charge in an ideal metal medium is also a point charge, and the two point charges cancel out each other.

As a consequence, when one applies the ESM method to a scheme based on the NAP method, there is no necessity to change the two energy terms, E_{na} and E_{scc}. The difference electron–electron Coulomb energy $E_{\delta ee}$, on the other hand, contributes to the total energy constructed from a long-range term δV_H, and is the only energy term influenced by the ESM boundaries. In this case, δV_H is reformulated using the corresponding Green's function as follows:

$$\delta V_H(\mathbf{r}) = \int d\mathbf{r}' G(\mathbf{r}, \mathbf{r}') \delta n(\mathbf{r}'). \tag{10}$$

The reformulation for the Hartree potential as shown in Eq. (10) is separated from the scheme of solving the eigenvalue problem. Therefore, if an O(N) method is adopted, the linear scalability of the O(N) calculations combined with the ESM method does not change.[20] It should be noted that simplifying the implementation of the ESM method using NAP is not only valid for the PAO basis functions used here, but also for any basis functions including the plane wave basis functions.

C. PAO basis functions

In our implementation of DFT, the KS orbitals have been expanded by a linear combination of optimized PAO basis functions which have been generated by a variational optimization method[6,11] and is non-zero within a cutoff radius r_c. Due to the locality of PAO, one may make zero matrix elements and the memory size increases linearly with the size of a calculation model. Then it makes O(N) calculations possible with good parallel efficiency when employing an O(N) eigenvalue solution such as the Krylov subspace method.[5]

It is generally known that when electronic structures are calculated using atomic local basis sets, BSSE can be a significant concern, especially in descriptions of molecular interactions. There are a number of possible ways to reduce the error: one is to use the BSSE correction schemes such as a counterpoise method,[21,22] and another is to use a large number of orbitals or to use orbitals optimized in advance. In the case of MD calculations, using the counterpoise method requires additional calculations at every time step and the use of a large number of orbitals can be very time consuming. In the present study, a variational optimization method based on the force theorem has been used.[6] Variational optimization of basis functions was performed for a set of model systems that accurately represent the chemical environments under consideration. Similar schemes have been successfully employed to reduce BSSE in the descriptions of molecular interactions.[12,13] A relatively small number of PAOs optimized with the method can reproduce convergent results obtained from a larger number of unoptimized PAOs. By adopting optimized PAO basis sets, therefore, it is possible to realize higher accuracy and larger scale O(N) simulations as shown later.

D. Force calculation under ESM boundaries

In a NAP-based calculation scheme, the forces on atoms are calculated from the derivative of each energy term with respect to the atom positions without an Ewald summation.[7–9] As mentioned in Sec. II B, the $E_{\delta ee}$ term has been modified

with the introduction of the ESM method to the NAP-based scheme. It follows that in the force calculation procedure with ESM boundaries, only the derivative of the difference Hartree energy $E_{\delta ee}$, $\partial E_{\delta ee}/\partial \mathbf{R}_k$, where $\mathbf{R}_k$ is the coordinate of the kth atom, should be considered as presented below.

By introducing a regular mesh in real space for the discretization of the numerical integration associated with the Hartree energy $E_{\delta ee}$,[8,9] the derivative of the difference Hartree energy $E_{\delta ee}$ is given by two parts including n or $n^{(a)}$ as

$$\frac{\partial E_{\delta ee}}{\partial \mathbf{R}_k} = \sum_p \frac{\partial n(\mathbf{r}_p)}{\partial \mathbf{R}_k} \frac{\partial E_{\delta ee}}{\partial n(\mathbf{r}_p)} + \sum_p \frac{\partial n^{(a)}(\mathbf{r}_p)}{\partial \mathbf{R}_k} \frac{\partial E_{\delta ee}}{\partial n^{(a)}(\mathbf{r}_p)}, \tag{11}$$

where $\mathbf{r}_p$ represents the pth grid point in real space. When Green's function expressing the boundary conditions in the ESM method is given as $G(\mathbf{r},\mathbf{r}')$, the difference Hartree potential $\delta V_H(\mathbf{r})$ can be expressed as

$$\delta V_H(\mathbf{r}) = \int d\mathbf{r}' G(\mathbf{r},\mathbf{r}')\delta n(\mathbf{r}'). \tag{12}$$

Equation (12) is rewritten as a real space expression as

$$\delta V_H(\mathbf{r}_p) = \Delta V \sum_q G(\mathbf{r}_p,\mathbf{r}_q)\delta n(\mathbf{r}_q) \tag{13}$$

with

$$\Delta V = \frac{1}{N_1 N_2 N_3}, \tag{14}$$

where N_1, N_2, and N_3 are the numbers of division on the $\boldsymbol{a}$, $\boldsymbol{b}$, and $\boldsymbol{c}$ axes in the real space unit cell, respectively. The derivative of $\delta V_H(\mathbf{r})$ with respect to $n(\mathbf{r})$ is

$$\begin{aligned}\frac{\partial \delta V_H(\mathbf{r}_p)}{\partial n(\mathbf{r}_q)} &= \frac{\partial}{\partial n(\mathbf{r}_q)} \left\{ \Delta V \sum_{q'} G(\mathbf{r}_p,\mathbf{r}_{q'})\delta n(\mathbf{r}_{q'}) \right\} \\ &= \frac{\partial}{\partial n(\mathbf{r}_q)} \left\{ \Delta V \sum_{q'} G(\mathbf{r}_p,\mathbf{r}_{q'})(n(\mathbf{r}_{q'}) - n^{(a)}(\mathbf{r}_{q'})) \right\} \\ &= \Delta V G(\mathbf{r}_p,\mathbf{r}_q). \end{aligned} \tag{15}$$

In the same way, we can obtain the derivative of $\delta V_H(\mathbf{r})$ with respect to $n^{(a)}(\mathbf{r})$ as

$$\frac{\partial \delta V_H(\mathbf{r}_p)}{\partial n^{(a)}(\mathbf{r}_q)} = -\Delta V G(\mathbf{r}_p,\mathbf{r}_q). \tag{16}$$

$E_{\delta ee}$ can be written in a discretized form with a regular mesh as

$$E_{\delta ee} = \frac{1}{2}\Delta V \sum_p \delta n(\mathbf{r}_p)\delta V_H(\mathbf{r}_p). \tag{17}$$

Here, let us consider the Green function expression for $\partial E_{\delta ee}/\partial n$ in Eq. (11),

$$\begin{aligned}\frac{\partial E_{\delta ee}}{\partial n(\mathbf{r}_q)} &= \frac{\partial}{\partial n(\mathbf{r}_q)} \left\{ \frac{1}{2}\Delta V \sum_p \delta n(\mathbf{r}_p)\delta V_H(\mathbf{r}_p) \right\} \\ &= \frac{\partial}{\partial n(\mathbf{r}_q)} \left\{ \frac{1}{2}\Delta V \sum_p (n(\mathbf{r}_p) - n^{(a)}(\mathbf{r}_p))\delta V_H(\mathbf{r}_p) \right\} \\ &= \frac{1}{2}\Delta V \left\{ \delta V_H(\mathbf{r}_q) + \sum_p \delta n(\mathbf{r}_p) \frac{\partial \delta V_H(\mathbf{r}_p)}{\partial n(\mathbf{r}_q)} \right\} \\ &= \frac{1}{2}\Delta V \delta V_H(\mathbf{r}_q) + \frac{\Delta V^2}{2} \sum_p G(\mathbf{r}_p,\mathbf{r}_q)\delta n(\mathbf{r}_p) \\ &= \frac{1}{2}\Delta V \delta V_H(\mathbf{r}_q) + \frac{1}{2}\Delta V \delta V_H(\mathbf{r}_q) = \Delta V \delta V_H(\mathbf{r}_q). \end{aligned} \tag{18}$$

For $\partial E_{\delta ee}/\partial n^{(a)}$, we can obtain the derivative in the same way as

$$\frac{\partial E_{\delta ee}}{\partial n^{(a)}(\mathbf{r}_q)} = -\Delta V \delta V_H(\mathbf{r}_q). \tag{19}$$

As a consequence, the equations of the NAP forces with ESM boundaries, Eq. (18) and (19), do not include $G(\mathbf{r},\mathbf{r}')$ and are in the exactly same forms as the equation derived for the case of no ESM.[7–9] It indicates that even when one introduces ESMs to a NAP-based scheme, it is not necessary to change the original force calculation, resulting in a simple implementation of the ESM method.

III. PROOF CALCULATIONS

We have implemented the ESM method into an O(N)-DFT code, OpenMX (Open source package for Material eXplorer).[23] In OpenMX, the O(N) computation based on the Krylov subspace method is implemented with the PAO basis functions and the NAP scheme. Here, the precision of the electronic structure calculations obtained with the combined scheme of ESM, PAO, and NAP methods was demonstrated through several simple calculations.

First of all, we checked the total energies and several energy terms of an 1 × 1 Al-terminated Si(111) slab computed using an ordinary repeated slab (RS) and a slab between two semi-infinite vacuum regions as ESMs (isolated slab (IS)). For non-NAP-based schemes, the values of the Hartree, local-part, and core–core interaction energies are affected simultaneously by the existence of the ESM boundaries and are different from the original values obtained in the RS model because of the different treatments of the diverging term, $\mathbf{G}_{\|} = 0$. The sum of these energies is identical in both the RS and IS cases.[1] In our case, on the other hand, the only term affected by the ESM boundaries is $E_{\delta ee}$. It indicates that in a NAP-based scheme, as long as ESMs are located appropriately in the calculation system to obtain the correct wave functions, every energy term should be identical for the RS and IS calculations. This proof calculation was carried out using a local density approximation[24,25] within DFT. The cutoff

TABLE I. Comparison of energies calculated for Al-Si(111). RS: repeated slab; IS: isolated slab with the two semi-infinite vacuum regions as ESMs. The unit of energy is hartree.

	$E_{\rm kin}$	$E_{\rm xc}$	$E_{\delta \rm ee}$	$E_{\rm total}$
RS	93.7071469	−22.9685531	0.0765968	−127.3568720
IS	93.7071486	−22.9685553	0.0765968	−127.3568721

energy of 150 Ry was used, and double valence plus polarization function basis sets with $r_{\rm c} = 7.5$ bohrs were used for both kinds of atoms. The structure parameters of the Al-Si(111) slab were the same as those used in Ref. 1. The width of the vacuum region between the Al-termination and the cell-edge (the position of the ESMs) was 10 Å. Table I presents our computations and shows the agreement between the total energies for the IS and RS system within an accuracy of 10^{-6} hartree. The kinetic and exchange-correlation energies, $E_{\rm K}$ and $E_{\rm xc}$, have also been obtained for the two calculation cases with an accuracy of 10^{-5} hartree, which means that the electronic wave functions (electron densities) were fundamentally identical in both the calculations. With regard to $E_{\delta \rm ee}$, the accuracy was on the order of 10^{-7} hartree.

Next, to examine the accuracy of the electronic structure of a charged slab with ESM boundaries, the calculation results for such a slab were compared with those reported in Ref. 1. In this test, the same slab model as above was located between vacuum and ideal metal boundaries. The bias induced differences in the planar average of the valence charge density $\Delta\rho$ and the electrostatic potential ΔV obtained with our scheme are in good agreement with Fig. 3(b) of Ref. 1.

As the last test, the reliability of the implementation of force calculations with ESM boundaries has been checked by comparing the values of analytic and numerical forces. These check calculations were carried out on the same Al-Si(111) slab model as used above. The numerical force values were obtained by shifting the atom positions by 10^{-4} bohrs. The difference between the analytic and numerical forces was calculated to be less than 10^{-4} hartree/bohr, which shows the reliability of the force calculation with ESM boundaries.

IV. APPLICATION TO MD SIMULATION

As a demonstration of a large-scale O(N) calculation using the ESM method, MD simulations were performed on the interface of a H-terminated Si(111) electrode and propylene carbonate ($C_4H_6O_3$; PC) solvent. Silicon-based materials have attracted much attention and been intensively investigated as an attractive candidate for an anode in high-capacity Li-ion secondary batteries (LIBs) because of its tremendously high Li-storage capacity,[26] while PC is a solvent thought to have used in such a Si-based anode in LIBs.[27]

In the model, a hydrogen-terminated 4 × 4 Si(111) slab consisting of 96 Si and 32 H atoms, and 20 PC molecules were included (388 atoms) in the unit cell under periodic boundary conditions. The cell was 13.30, 15.36, and 38.0 Å in size as shown in Fig. 2.

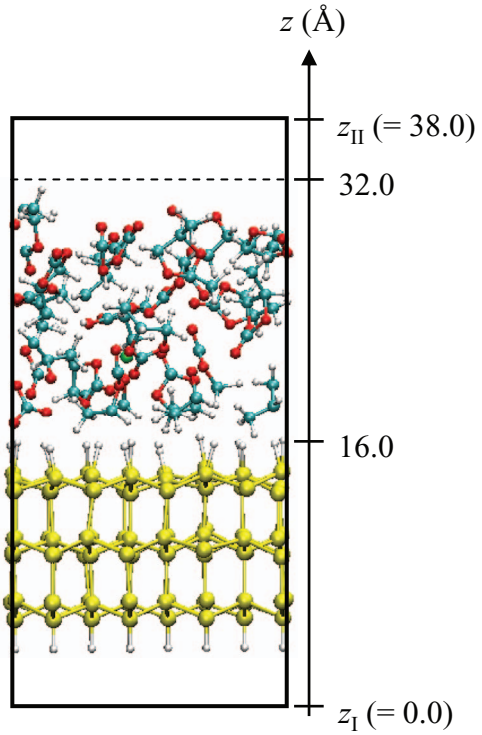

FIG. 2. Unit cell of the demonstration simulation model for a H-Si(111) anode and propylene carbonate solvent interface (solid outer rectangle). ESMs, semi-infinite vacuum and ideal metal, were placed at $z \le z_{\rm I}$ (= 0.0 Å) and $z \ge z_{\rm II}$ (= 38.0 Å), respectively. An artificial potential wall (dashed line) was set at z = 32.0 Å. The average z-coordinate of the H-layer contacting the PC solvent was 16.0 Å.

As ESMs, a semi-infinite continuum with an infinite dielectric constant (ideal metal) was located beyond the upper edge of the cell ($z \ge 38.0$ Å), while a semi-infinite vacuum was located at $z \le 0$ (see Fig. 2). To simulate H-Si(111) as an LIB-anode, the electric bias was imposed by introducing excess electrons to the system with the opposite image charge in the ideal-metal ESM. During the MD simulation, the excess charge, $N_{\rm ex}$, was increased with time as indicated in Table II. The value of imposed bias between the semi-infinite vacuum and center of the solvent was estimated to be about 0.7 V for $N_{\rm ex} = 0.55$ electron.[28]

DFT calculations were performed using a generalized gradient approximation.[29] The energy cutoff of 170 Ry was used for the numerical integrations, and the Γ point in k-space was employed for the Brillouin zone sampling. The molecular dynamics calculations were carried out in a *NVT* ensemble at 600 K. Velocities of atoms were scaled every 50 MD steps to keep the temperature constant.[30] The time-step width was 1.2 fs with substitution of the deuterium mass for hydrogen atoms. The positions of the bottom H and the lowest Si atoms were fixed during the MD calculations.

TABLE II. Number of excess electrons doped into the H-Si(111)-PC interface model ($N_{\rm ex}$) at MD times.

MD time (fs)	0.0–240	241.2–595.2	596.4–1495.2	1496.4–1600.8
$N_{\rm ex}$	0.25	0.35	0.45	0.55

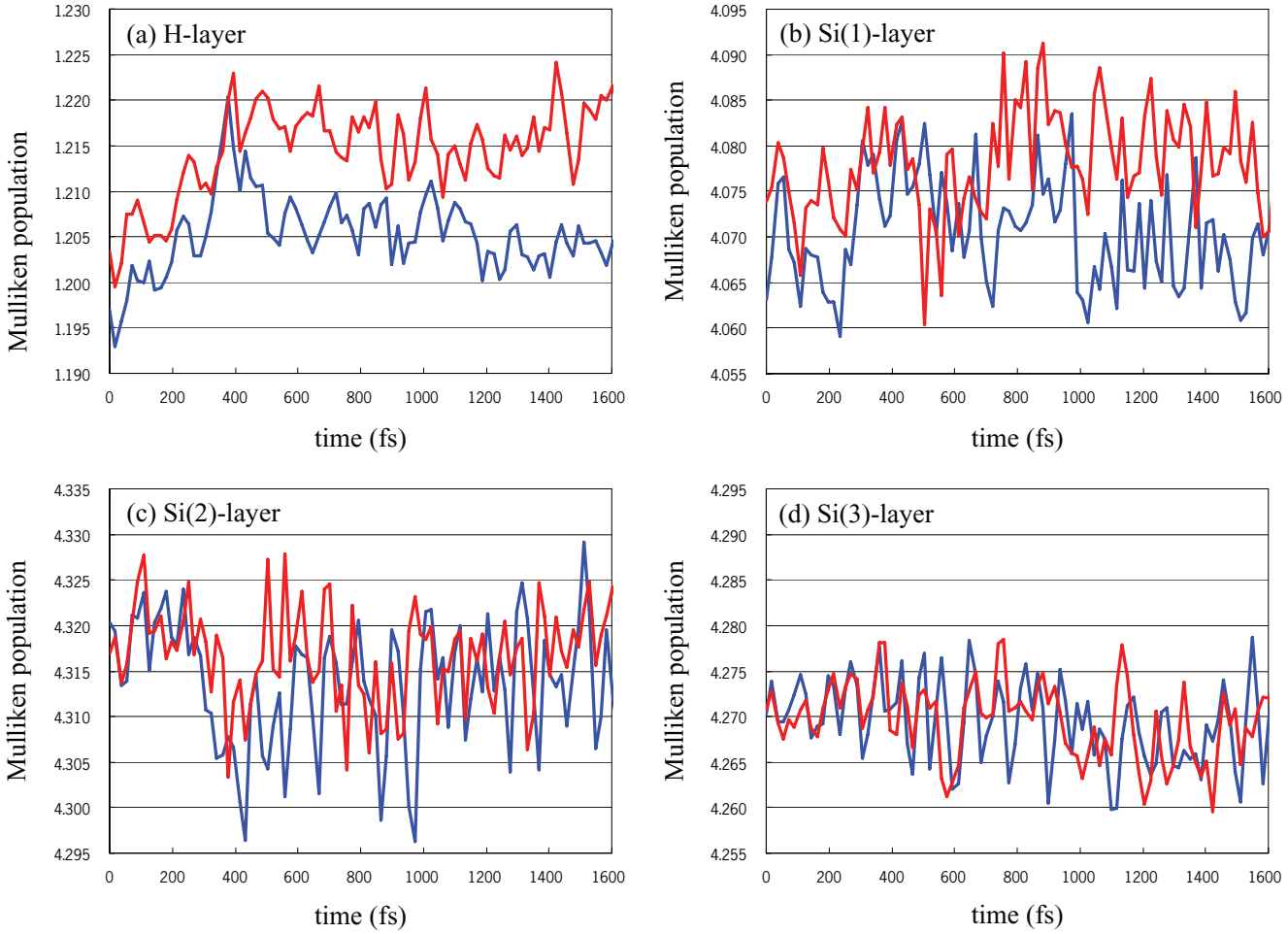

FIG. 3. (a)–(d) Mulliken populations of the valence electrons in the surface layers of a H-Si(111) slab. Red line: charged surface; blue line: uncharged surface. The population value has been averaged over all the atoms in each layer, every 18 fs.

The basis sets adopted on moving atoms during the MD runs were double valence plus single-polarization types, $s2p1$ and $s2p2d1$, for H and the other atoms, respectively. For fixed atoms, double valence basis sets were used. The cutoff radii of the basis sets were 8.0 and 7.0 bohrs for Si and the other atoms, respectively. All basis sets and pseudopotentials were adopted from the OpenMX Database version 2011.[14] With regard to the basis sets placed on the PC molecules, the optimizations of the PAO basis functions[6] were carried out in order to reduce BSSE between the PC molecules.[31] The interaction energy between two PC molecules through C–H$\cdots$O=C as calculated using the optimized basis sets explained above was 4.15 kcal/mol, which is comparable to the value obtained with a plane-wave-based calculation (4.04 kcal/mol).[32] The BSSE between two PC molecules estimated with the counterpoise method was 1.06 kcal/mol, which improved with orbital optimization to be 0.69 kcal/mol. This was then within the chemical accuracy of 1.0 kcal/mol.

The O(N) calculations were carried out using the Krylov subspace method.[5] The Krylov-method parameters used in the O(N) calculations were determined so as to guarantee a precision of about 10^{-5} and 10^{-4} hartree/atom in the total energy compared to the results by the exact diagonalization for the PC-bulk and Si-slab parts, respectively.

The charge distribution in the electrode induced by excess negative charge was then investigated to confirm our O(N) scheme with ESM works well. Figure 3 shows the decrease in the Mulliken populations of the valence electrons in the H and Si(1) layers on the solvent side of the slab after doping with excess electrons. The Mulliken populations of the valence electrons on the electrode inside, Si(2)- and Si(3) layers, on the other hand, seem to undergo no change. These results show that the segregation of excess electrons at the electrode surface was realized successfully with the ESM method, as already observed.[3,4]

Next, the bias-induced changes of the interface structure of the PC solvent will be discussed. Figure 4 shows the PC molecule distribution functions $g_\gamma(z)$ with and without the introduced excess charge. The centroid of the ring of each PC molecule was used as a representative position of the molecule. In both the cases, two peaks in $g_\gamma(z)$ are found to be around 3.5–4.5 and 8.0–9.5 Å from the surface ($z = 19.5$–20.5 and 24.0–25.5 Å, respectively). Hereafter the former region shall be referred to as the "contact" region and the latter as the "bulk" region. The two regions are separated at the minimal point between two peaks, at $z = 22.0$ Å. The PC molecules are structured near the surface as is generally observed in solid–liquid interfaces. The similar molecule orientation has been

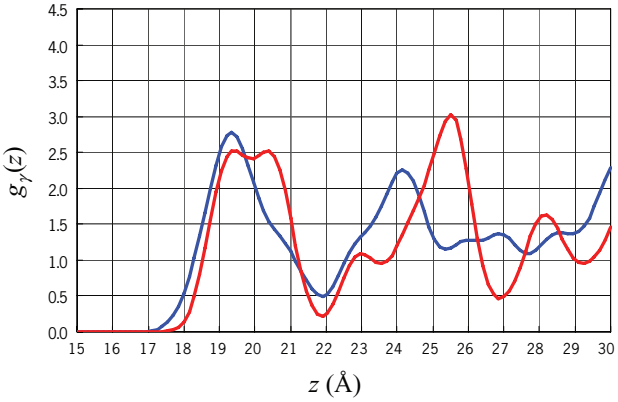

FIG. 4. Propylene carbonate distribution functions $g_\gamma(z)$ for uncharged and charged surfaces. Red line: charged surface; blue line: uncharged surface. The representative point for the PC molecules is the centroid of the five-membered ring. The average z-coordinate of the H-layer contacting the PC solvent is at 16.0 Å.

observed on Pt and water interface with an electric bias.[33] By adding the bias, the two peaks nearest to the electrode surface ($z = 19.5$ and 24.0 Å) shifted in the $+z$ direction.

Figures 5 and 6 show the distribution functions of methyl group (hydrogen and carbon atoms) and carbonyl group (oxygen and carbon atoms), respectively. Figure 5 indicates that the distribution of C atoms in CH_3 overlaps with the wider distribution of H in CH_3. This suggests a random orientation

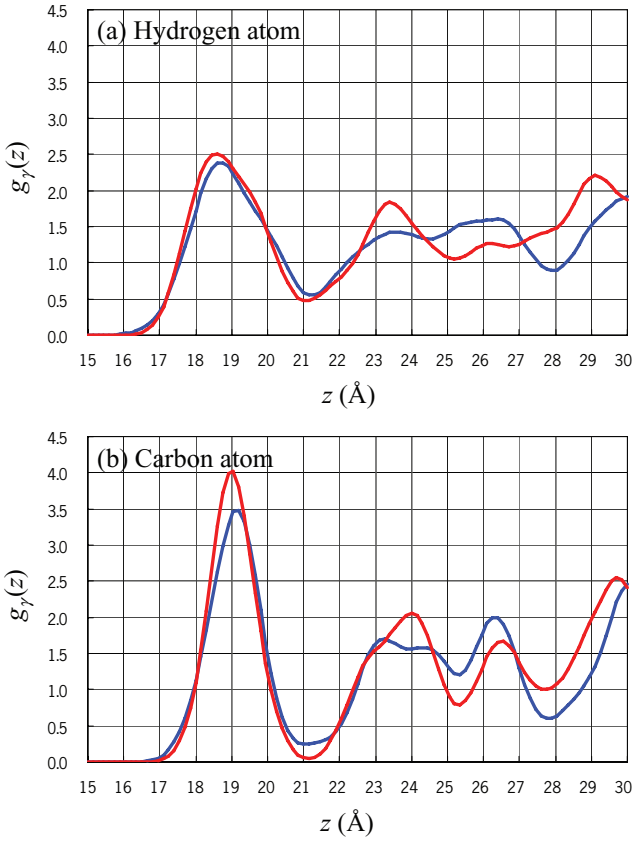

FIG. 5. Distribution functions $g_\gamma(z)$ of contacts between the H-Si(111) surface and the methyl group of PC molecule. (a) Hydrogen atom and (b) carbon atom. Red line: charged surface; blue line: uncharged surface. The average z-coordinate of the H-layer contacting the PC solvent is at 16.0 Å.

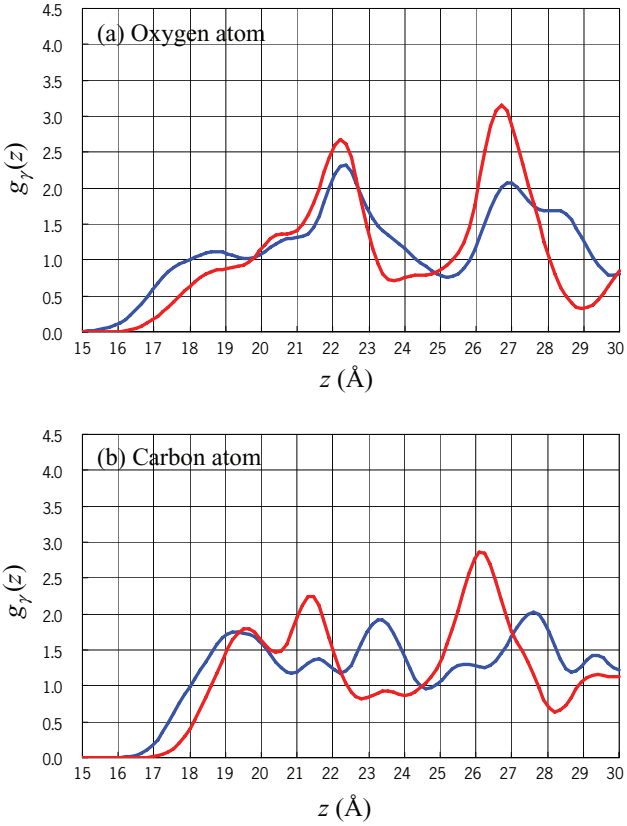

FIG. 6. Distribution functions $g_\gamma(z)$ of contacts between the H-Si(111) surface and the carbonyl group of the PC molecule. (a) oxygen atom and (b) carbon atom. Red line: charged surface; blue line: uncharged surface. The average z-coordinate of the H-layer contacting the PC solvent is at 16.0 Å.

of CH_3 with no ordered structure. The imposed electric field induces a small first-peak position shift in the contact region for both atoms. This may be caused by the attractive interactions between the negatively charged surface and positive methyl groups,[2] although the shifts are very small.

According to Fig. 6, the probability of a carbonyl group being near the surface ($z < 19$ Å) is reduced by the imposed electric field. This may be due to the repulsive interaction between the negatively charged surface and the negative charge of the carbonyl group. The distribution of the carbonyl oxygen has two peaks at $z = 22.5$ and 27.0 Å both with and without the electric field. By imposing an electric field, the distribution of carbonyl carbons has a distinct interface structure: two peaks at $z = 18.0$–22.0 Å and a sharp peak at $z = 26.0$ Å. By adding a bias, all the atom peaks of the carbonyl group become sharp. This implies that the electric bias makes the interface region more structured.

To elucidate effect of the electric field on the interface structure, focusing on the orientation of the PC molecules, we calculated the distribution functions of both the PC position and orientation $g(z, \theta)$.[33] Here z is the centroid of the C=O bond and θ is the angle between the surface normal vector (outgoing) and the dipole moment (from O to C) of a carbonyl bond (see Fig. 7). Figure 8 shows that the imposed electric field induces a high probability around $(z, \theta) = (22.0$ Å, 130°) and (20.0 Å, 120°), where the carbonyl groups in the contact

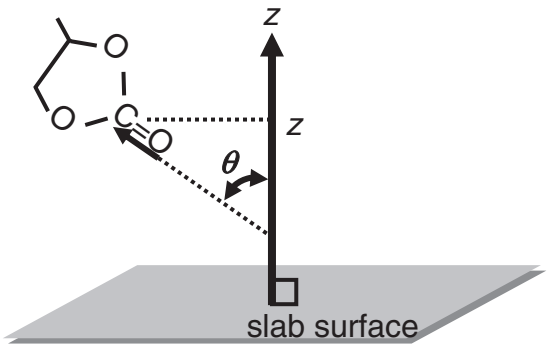

FIG. 7. Definitions of z and θ for the position and orientation of a PC molecule. The position z is the z-coordinate of the centroid of the carbonyl bond. θ is the angle between normal vector of the slab surface and dipole vector of the carbonyl bond.

region are aligned with the oxygen atoms pointing away from the surface to gain electric stabilization.

To summarize the MD calculations for the H-Si(111) anode and PC solvent interface, PC molecules screen the segregated excess charge on the electrode surface by altering the positions and orientations of carbonyl groups (the most strongly polarized functional group in PC molecule). Since the similar change of molecule orientation has been observed on Pt and water interface with an electric bias,[33] the present scheme may be considered to be useful for simulation of the electrochemical systems. Further experimental observations for such a complex interface would be of interest.

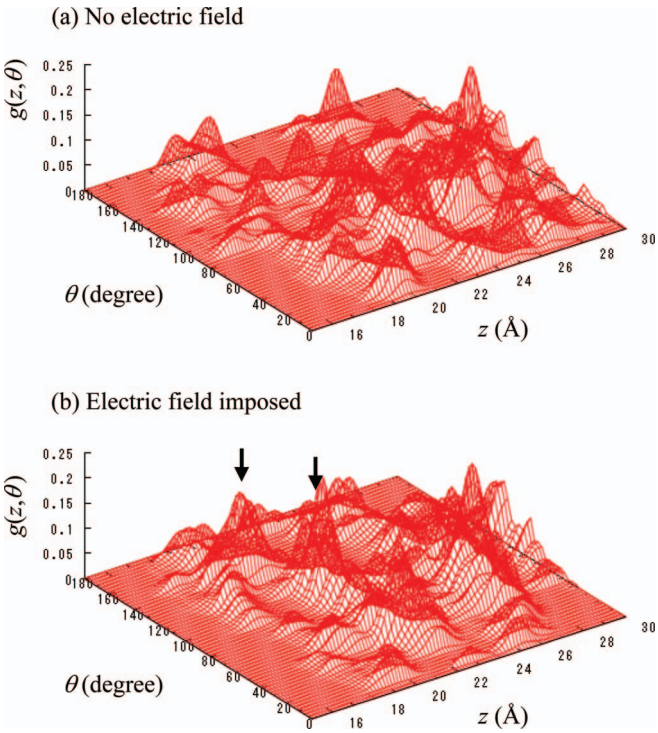

FIG. 8. (a) and (b) Probability distribution functions of PC position and the orientation $g(z,\theta)$. Arrows in (b) indicate peaks appearing due to an imposed electric field.

V. CONCLUSIONS AND PERSPECTIVES

To achieve large-scale first-principles MD calculations on electrochemical systems, the ESM method has been introduced to an O(N) DFT-calculation scheme based on the NAP scheme and the Krylov subspace method. Using this method, it is unnecessary to modify the force calculation procedure from the known NAP scheme. The precision of this implementation has been confirmed by test calculations for energy and force. To demonstrate the applicability of our method to large-scale calculations, MD simulations on an interface between a negatively charged H-Si(111) anode and PC solvent have been presented. The segregation of excess charge on the electrode surface and the change in the structure of the PC solvent in the interface has been observed. In order to carry out higher precision simulations of structure at the interface including large solvent molecules such as PC, further MD calculations should be performed with the larger models and longer time scales than the present calculations. Our demonstrative calculations have shown the applicability of the ESM method combined with the O(N) method for large-scale simulations of electrochemical systems with bandgaps varying according to the imposed bias. Several thousand atom MD simulations with highly parallel processing will be possible for either, metal or semi-conductor electrodes.

ACKNOWLEDGMENTS

The computation in this work was performed using computers at the Information Initiative Center, Hokkaido University, and the Research Center for Advanced Computing Infrastructure, Japan Advanced Institute of Science and Technology (JAIST). T.O. would like to acknowledge the financial support of the New Energy and Industrial Technology Development Organization (NEDO) of Japan and Professor M. Omiya (Hokkaido University) for supporting our implementation of OpenMX at the supercomputer of Hokkaido University.

[1] M. Otani and O. Sugino, Phys. Rev. B **73**, 115407 (2006).
[2] O. Sugino, I. Hamada, M. Otani, Y. Morikawa, T. Ikeshoji, and Y. Okamoto, Surf. Sci. **601**, 5237 (2007).
[3] M. Otani, I. Hamada, O. Sugino, Y. Morioka, Y. Okamoto, and T. Ikeshoji, J. Phys. Soc. Jpn. **77**, 024802 (2008).
[4] C. D. Taylor, S. A. Wasileski, J.-S. Filhol, and M. Neurock, Phys. Rev. B **73**, 165402 (2006).
[5] T. Ozaki, Phys. Rev. B **74**, 245101 (2006), and references therein.
[6] T. Ozaki, Phys. Rev. B **67**, 155108 (2003).
[7] O. F. Sankey and D. J. Niklewski, Phys. Rev. B **40**, 3979 (1989).
[8] J. M. Soler, E. Artacho, J. D. Gale, A. Garcia, J. Junquera, P. Ordejon, and D. Sanchez-Portal, J. Phys.: Condens. Matter **14**, 2745 (2002).
[9] T. Ozaki and H. Kino, Phys. Rev. B **72**, 045121 (2005).
[10] A. S. Torralba, M. Todorović, V. Brázdová, R. Choudhury, T. Miyazaki, M. J. Gillan, and D. R. Bowler, J. Phys.: Condens. Matter **20**, 294206 (2008).
[11] T. Ozaki and H. Kino, Phys. Rev. B **69**, 195113 (2004).
[12] J. V. Vondele and J. Hutter, J. Chem. Phys. **127**, 114105 (2007).
[13] V. Blum, R. Gehrke, F. Hanke, P. Havu, V. Havu, X. Ren, K. Reuter, and M. Scheffler, Comput. Phys. Commun. **180**, 2175 (2009).
[14] T. Ozaki, "Accurate LCPAO method for large-scale density functional calculations" (unpublished).
[15] The corresponding Green's function is formulated in the Laue representation, $G(\mathbf{G}_{\parallel}, z)$, where $\mathbf{G}_{\parallel}$ is a wave vector parallel to the surface.

[16]For example, J. V. Vondele, M. Krack, F. Mohamed, M. Parrinello, T. Chassaing, and J. Hutter, Comput. Phys. Commun. **167**, 103 (2005).
[17]N. Troullier and J. L. Martine, Phys. Rev. B **43**, 1993 (1991).
[18]I. Morrison, D. M. Bylander, and L. Kleinman, Phys. Rev. B **47**, 6728 (1993).
[19]In ESM method approach, boundaries of the Poisson's equation, $z = z_{\rm I}$ and $z_{\rm II}$, should be located in region which is far enough from any atom positions so that no charge penetrates into the media.
[20]With regard to the linear scalability of calculation based on Krylov subspace method, adopted as an O(N) scheme in the presented scheme, see Ref. 5.
[21]S. F. Boys and F. Bernardi, Mol. Phys. **19**, 553 (1970).
[22]S. Simon, M. Duran, and J. J. Dannenberg, J. Chem. Phys. **105**, 11024 (1996).
[23]See http://www.openmx-square.org/ for the code, OpenMX, pseudo-atomic basis functions and pseudopotentials.
[24]D. M. Ceperley and B. J. Alder, Phys. Rev. Lett. **45**, 566 (1980).
[25]J. P. Perdew and A. Zunger, Phys. Rev. B **23**, 5048 (1981).
[26]U. Kasavajjula, C. Wang, and A. J. Appleby, J. Power Sources **163**, 1003 (2007), and references therein.
[27]S. Ohara, J. Suzuki, K. Sekine, and T. Takamura, J. Power Sources **119-121**, 591 (2003).
[28]In Ref. 3, the electrode potential is calculated from the potential of the semi-infinite vacuum region relative to the time-averaged electrostatic potential in the water region with a flat profile. Our electrically biased model system, however, was still in relaxation process during doping excess electrons until $N_{\rm ex} = 0.45$ e, and the flat potential profile in the bulk of the relaxed PC solvent region was obtained around 1.7 ps after starting doping excess electrons ($N_{\rm ex} = 0.55$ e), whereby we could not obtain the time-averaged electrostatic potential of the solvent region for $N_{\rm ex} = 0.25$ to 0.45 e. Therefore, the representative value of voltage was estimated by using the potential of the PC solvent bulk at 1.8 ps.
[29]J. P. Perdew, K. Burke, and M. Ernzerhof, Phys. Rev. Lett. **77**, 3865 (1996).
[30]L. V. Woodcock, Chem. Phys. Lett. **10**, 257 (1971).
[31]In our basis-set optimizations, each set of double valence was constructed from eight primitive orbitals, and each polarization function also from eight primitive orbitals. The cutoff energy of the orbital optimization was 170 Ry, and the threshold was 10^{-5} (hartree/bohr)^2.
[32]The optimized structure and the reference value of stabilized energy of PC–PC interaction system was obtained by CASTEP version 4.3 with GGA-PBE and ultrasoft pseudopotentials. The energy cutoff of 300 eV and the G point in k-space was employed for the cell of $20 \times 20 \times 20$ Å^3.
[33]M. Otani, I. Hamada, O. Sugino, Y. Morioka, Y. Okamoto, and T. Ikeshoji, Phys. Chem. Chem. Phys. **10**, 3609 (2008).